Long-Wavelength Analysis of Plane Wave Irradiation of a Prolate Spheroid Model of Man

CARL H. DURNEY, MEMBER, IEEE, CURTIS C. JOHNSON, SENIOR MEMBER, IEEE, AND HABIB MASSOUDI

Abstract—**An electromagnetic (EM) field perturbation technique is used to find internal electrical fields and the absorbed power of a prolate spheroid being irradiated by a plane wave when the wavelength is long compared to the dimensions of the spheroid. The results show significant differences in the power absorption patterns with changes in the orientation of the spheroid with respect to the incident EM fields. Calculations of the power absorbed by a prolate spheroid model of man are given.**

I. INTRODUCTION

In the investigation of electromagnetic (EM) power absorption in man, it would be desirable to perform a rigorous theoretical analysis corroborated by measurement of electric field intensity at any specified tissue site in the body. As a first step in this direction, a tissue sphere has been analyzed by Johnson and Guy [1], Anne *et al.* [2], Shapiro *et al.* [3], Kritikos and Schwan [4], Lin *et al.* [5], and Joines and Spiegel [6]. Results of these analyses show that there can be large spatial variations in the electric field and absorbed power in the tissues as a function of sphere radius and frequency. These theoretical results have been confirmed by thermographic camera photographs of irradiated phantom models [1], [5]. Based on these indications, it is expected that tissue field and power deposition in man will vary greatly with frequency, body configuration, and orientation, thus complicating the quantification of EM power absorption. Yet obtaining knowledge of the details of internal power absorption is essential in order to extrapolate animal data as an indication of hazard to man.

This leads then to the urgent need for analytical tools to describe power absorption patterns in realistic models of man and experimental animals. A model more realistic than the sphere for the human body and many animal bodies is the prolate spheroid. A general field solution to the prolate spheroidal boundary problem is extremely difficult, but solutions for low ka are tractable using the perturbation theory described by Van Bladel [7]. One advantage of the perturbation theory is that it avoids solution of the EM wave equation and requires instead only the solution of equations which are similar to the static equations. This is a significant advantage because the mathematical functions in the solutions to the static equations are more familiar and easier to work with than the spheroidal functions. Another advantage of perturbation theory is that it lends itself more easily to physical interpretation of the results and allows easier generalization.

In this paper, the perturbation theory is first described and the results for a sphere [7] compared to the approximate Mie theory of Lin *et al.* [5]. Then the perturbation technique is systematically applied to analyze the internal fields in a prolate spheroid irradiated by a plane wave for each of the three major orientations of the incident fields with respect to the spheroid. Curves of power absorption versus frequency show that the absorbed power is a strong function of orientation of the spheroid in the incident fields.

Manuscript received April 5, 1974; revised September 3, 1974. This work was supported by the USAF School of Aerospace Medicine, Brooks Air Force Base, Tex. 78235.

C. H. Durney and H. Massoudi are with the Department of Electrical Engineering, the University of Utah, Salt Lake City, Utah 84112.

C. C. Johnson is with the Department of Biophysics and Bioengineering, the University of Utah, Salt Lake City, Utah 84112.

II. DESCRIPTION OF THE PERTURBATION THEORY

The method outlined here follows closely that of Van Bladel [7]. The situation considered is that of an incident wave impinging upon a scattering body, as shown in Fig. 1. The basis of the perturbation theory is the expansion of each set of fields, interior, incident, and scattered, in a powers series in $-jk$, where k is the free-space propagation constant. Accordingly, we write

$$\mathbf{E} = \sum_{n=0}^{\infty} \mathbf{E}_n(-jk)^n$$

$$\mathbf{E}^i = \sum_{n=0}^{\infty} \mathbf{E}_n{}^i(-jk)^n$$

$$\mathbf{E}^s = \sum_{n=0}^{\infty} \mathbf{E}_n{}^s(-jk)^n$$

where $\mathbf{E}$, $\mathbf{E}^i$, and $\mathbf{E}^s$ are the interior, incident, and scattered fields, respectively, with similar expressions for the magnetic fields. Each set of fields must satisfy Maxwell's equations. Thus the interior fields must satisfy

$$\nabla \times \mathbf{E} = \eta_0(-jk)\mathbf{H}$$

$$\nabla \times \mathbf{H} = \sigma\mathbf{E} - \frac{(-jk)\epsilon_r}{\eta_0}\mathbf{E}$$

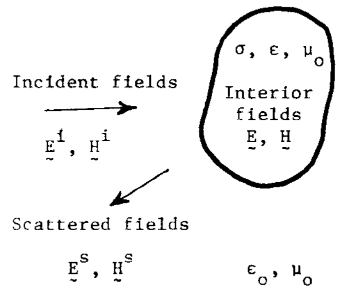

Fig. 1. The basic situation treated in this paper, an incident wave impinging upon a scatterer resulting in scattered fields.

$$\nabla \cdot \mathbf{H} = 0$$

$$\nabla \cdot \left(\sigma \mathbf{E} - \frac{(-jk)\epsilon_r}{\eta_0} \mathbf{E} \right) = 0$$

where

$$\eta_0 = (\mu_0/\epsilon_0)^{1/2}$$
$$k = \omega(\mu_0\epsilon_0)^{1/2}$$
$$\epsilon_r = \epsilon/\epsilon_0 \qquad \text{(real)}$$

and $\exp(j\omega t)$ time variation has been assumed.

Substituting the series expansions for $\mathbf{E}$ and $\mathbf{H}$ into these equations and equating coefficients of like powers of $-jk$ results in the following set of equations

$$\nabla \times \mathbf{E}_0 = 0 \tag{1}$$

$$\nabla \times \mathbf{E}_n = \eta_0 \mathbf{H}_{n-1} \qquad n \geq 1 \tag{2}$$

$$\nabla \times \mathbf{H}_0 = \sigma \mathbf{E}_0 \tag{3}$$

$$\nabla \times \mathbf{H}_n = \sigma \mathbf{E}_n - \frac{\epsilon_r}{\eta_0} \mathbf{E}_{n-1} \qquad n \geq 1 \tag{4}$$

$$\nabla \cdot \mathbf{E}_0 = 0 \tag{5}$$

$$\nabla \cdot \left(\sigma \mathbf{E}_n - \frac{\epsilon_r}{\eta_0} \mathbf{E}_{n-1} \right) = 0 \qquad n \geq 1 \tag{6}$$

$$\nabla \cdot \mathbf{H}_n = 0. \tag{7}$$

Following a similar procedure for the scattered fields results in

$$\nabla \times \mathbf{E}_0^s = 0 \tag{8}$$

$$\nabla \times \mathbf{E}_n^s = \eta_0 \mathbf{H}_{n-1}^s \tag{9}$$

$$\nabla \times \mathbf{H}_0^s = 0 \tag{10}$$

$$\nabla \times \mathbf{H}_n^s = -\frac{1}{\eta_0} \mathbf{E}_{n-1}^s \tag{11}$$

$$\nabla \cdot \mathbf{E}_n^s = 0 \tag{12}$$

$$\nabla \cdot \mathbf{H}_n^s = 0. \tag{13}$$

The power-series expansion for the incident fields is assumed to be known.

With the restriction that the scatterer is nonmagnetic, the boundary conditions are

$$\hat{\mathbf{n}} \cdot \left(\sigma - \frac{(-jk)\epsilon_r}{\eta_0} \right) \mathbf{E} = \hat{\mathbf{n}} \cdot \left(-\frac{-jk}{\eta_0} \right) (\mathbf{E}^i + \mathbf{E}^s)$$

$$\hat{\mathbf{n}} \times \mathbf{E} = \hat{\mathbf{n}} \times (\mathbf{E}^i + \mathbf{E}^s)$$

$$\mathbf{H} = \mathbf{H}^i + \mathbf{H}^s$$

where $\hat{\mathbf{n}}$ is the outer unit normal vector at the boundary. Substituting the power-series expansions into these boundary conditions and equating coefficients of like powers of $-jk$ gives us

$$\hat{\mathbf{n}} \cdot \mathbf{E}_0 = 0 \tag{14}$$

$$\hat{\mathbf{n}} \cdot \left(\sigma \mathbf{E}_n - \frac{\epsilon_r}{\eta_0} \mathbf{E}_{n-1} \right) = -\frac{\hat{\mathbf{n}}}{\eta_0} \cdot (\mathbf{E}_{n-1}^i + \mathbf{E}_{n-1}^s) \qquad n \geq 1 \tag{15}$$

$$\hat{\mathbf{n}} \times \mathbf{E}_n = \hat{\mathbf{n}} \times (\mathbf{E}_n^i + \mathbf{E}_n^s) \tag{16}$$

$$\mathbf{H}_n = \mathbf{H}_n^i + \mathbf{H}_n^s. \tag{17}$$

Along with the series expansion of the incident fields, equations (1)–(15) constitute the formulation of the problem. In addition, the conditions on the scattered fields at infinity must be known. Van Bladel [7] has shown that the first two terms in the expansion of the scattered fields are of order $1/r^2$ and hence vanish at infinity. Thus the formulation is complete, and the next step is to apply the perturbation method. Before investigating the power absorbed by a prolate spheroid, we shall briefly compare the results obtained by perturbation theory for a sphere with the results obtained by the long-wavelength approximation of the Mie theory.

Consider a plane wave with fields

$$\mathbf{E}^i = \exp(-jky)\hat{\mathbf{z}} = \sum_{n=0}^{\infty} \frac{(-jky)^n}{n!} \hat{\mathbf{z}} \tag{18}$$

$$\mathbf{H}^i = \frac{\exp(-jky)}{\eta_0} \hat{\mathbf{x}} = \frac{1}{\eta_0} \sum_{n=0}^{\infty} \frac{(-jky)^n}{n!} \hat{\mathbf{x}} \tag{19}$$

incident upon a sphere with conductivity σ and relative permittivity ϵ_r. $\hat{\mathbf{x}}$ and $\hat{\mathbf{z}}$ are unit vectors in the x and z directions, respectively.

The total first-order field inside the sphere as derived by Van Bladel [7] is

$$\mathbf{E} = \frac{3}{-j\sigma/\omega\epsilon_0} \hat{\mathbf{z}} + j\tfrac{1}{2}k(z\hat{\mathbf{y}} - y\hat{\mathbf{z}}). \tag{20}$$

From the long-wavelength approximation to the Mie theory [5], the approximate field inside the sphere is

$$\mathbf{E} = \frac{3}{\epsilon' - j\epsilon''} \hat{\mathbf{z}} + j\tfrac{1}{2}k(z\hat{\mathbf{y}} - y\hat{\mathbf{z}})$$

where $\epsilon' - j\epsilon''$ is the complex relative permittivity. Since $\epsilon'' = \sigma/\omega\epsilon_0$, the two expressions are equivalent when ϵ' is small enough compared to ϵ'' to be neglected, as it is in the case of typical biological tissue at lower frequencies. The difference between the two approximate values for the electric field apparently results from the difference in the methods of approximation. Numerical calculations for the sphere show that the results obtained by the perturbation theory are a good approximation to the exact results of the Mie theory for long wavelengths.

III. FIRST-ORDER FIELDS FOR THE PROLATE SPHEROID

In this section, the solution of the zeroth- and first-order equations for a plane wave incident on a prolate spheroid are described. Solutions are given for each of the three primary polarizations, and solutions for any polarization can be constructed from these. For convenience in referring to the three primary polarizations, the following definitions are made.

Magnetic polarization—the magnetic field vector of the incident plane wave is parallel to the major axis of the spheroid.

Electric polarization—the electric field vector of the incident plane wave is parallel to the major axis of the spheroid.

Cross polarization—the electric field vector and the magnetic field vector of the incident plane wave are both perpendicular to the major axis of the spheroid.

A. Magnetic Polarization

The coordinate system with respect to the prolate spheroid is oriented as shown in Fig. 2. The first polarization considered is magnetic polarization, in which the magnetic field of the incident plane wave is parallel to the major axis of the spheroid. Accordingly, the fields of the incident plane wave are chosen to be

$$\mathbf{E}^i = \exp(-jky)\hat{\mathbf{x}} = \hat{\mathbf{x}} \sum_{n=0}^{\infty} (-jky)^n/n! \tag{21}$$

$$\mathbf{H}^i = -\exp(-jky)\hat{\mathbf{z}}/\eta_0 = (-\hat{\mathbf{z}}/\eta_0) \sum_{n=0}^{\infty} (-jky)^n/n!. \tag{22}$$

The zeroth-order field must satisfy (1), (5), and (14), which are equivalent to the equations for the field inside a conducting spheroid in a uniform static electric field. The solution is $\mathbf{E}_0 = 0$. Similarly, $\mathbf{H}_0 = -\hat{\mathbf{z}}/\eta_0$, since the spheroid is nonmagnetic.

The electric field $\mathbf{E}_0^i + \mathbf{E}_0^s$ is the field resulting from the conducting spheroid in a uniform field. This solution will be found by using normalized prolate spheroidal coordinates (u_1,v_1,ϕ) defined by

$$u_1 = u/l$$

$$v_1 = v/l$$

where (u,v,ϕ) are the prolate spheroidal coordinates related to cylindrical coordinates (r,ϕ,z) by

$$r = (u^2 - l^2)^{1/2}(l^2 - v^2)^{1/2}/l \tag{23}$$

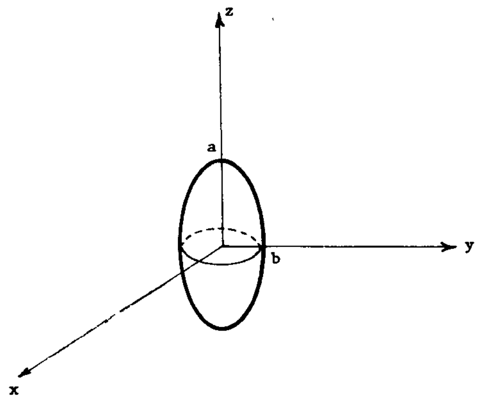

Fig. 2. Orientation of the coordinate system with respect to the prolate spheroid.

$$z = uv/l \tag{24}$$

$$\phi = \phi.$$

The spheroid is generated by revolving an ellipse about its major axis, and $2l$ is the distance between the foci of the ellipse. The major and minor axes are $2a$ and $2b$, respectively, and the eccentricity is $2l/2a$. The constant-u surfaces are ellipsoids of revolution and the constant-v surfaces are hyperboloids of revolution. Fig. 3 shows the unit vectors $\hat{\mathbf{u}}$ and $\hat{\mathbf{v}}$ at one point in the yz plane. The unit vector $\hat{\boldsymbol{\phi}}$ is the same as in a cylindrical coordinate system.

The unit vectors in spheroidal coordinates may be related to the unit vectors $\hat{\mathbf{x}}$, $\hat{\mathbf{y}}$, and $\hat{\mathbf{z}}$ in rectangular coordinates by [8]

$$\hat{\mathbf{u}} = \frac{1}{h_1}\frac{\partial \mathbf{r}}{\partial u} \tag{25}$$

$$\hat{\mathbf{v}} = \frac{1}{h_2}\frac{\partial \mathbf{r}}{\partial v} \tag{26}$$

$$\hat{\boldsymbol{\phi}} = \frac{1}{h_3}\frac{\partial \mathbf{r}}{\partial \phi} \tag{27}$$

where $\mathbf{r} = x\hat{\mathbf{x}} + y\hat{\mathbf{y}} + z\hat{\mathbf{z}}$ and h's are the scale factors given by

$$h_1 = \left|\frac{\partial \mathbf{r}}{\partial u}\right| \tag{28}$$

$$h_2 = \left|\frac{\partial \mathbf{r}}{\partial v}\right| \tag{29}$$

$$h_3 = \left|\frac{\partial \mathbf{r}}{\partial \phi}\right|. \tag{30}$$

In order to find $\mathbf{E}_1$,$\mathbf{E}_0^s$ must be found. This can be accomplished by following a procedure similar to that used by Van Bladel [7] to find the solutions for a dielectric spheroid in a uniform field. Since $\mathbf{E}_0^i = \hat{\mathbf{x}}$, $\mathbf{E}_0^i = -\nabla(-x)$ where $x = r\cos\phi = l\cos\phi[(u_1^2 - 1)(1 - v_1^2)]^{1/2}$. Thus we can set

$$\mathbf{E}_0^i + \mathbf{E}_0^s = -\nabla(\Phi_0^i + \Phi_0^s)$$

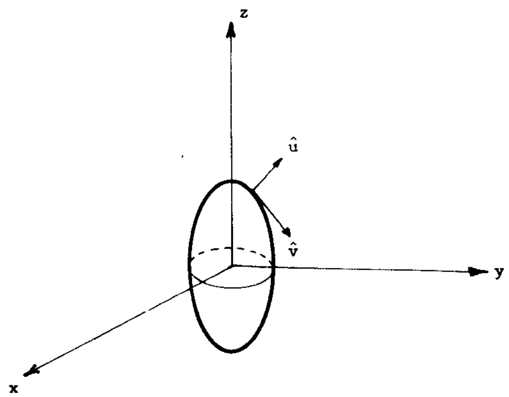

Fig. 3. The $\hat{\mathbf{u}}$ and $\hat{\mathbf{v}}$ vectors at one point in the yz plane.

where

$$\Phi_0{}^i = -l \cos\phi[(u_1{}^2 - 1)(1 - v_1{}^2)]^{1/2}$$

and $\Phi_0{}^s$ must satisfy Laplace's equation since $\nabla\cdot(\mathbf{E}_0{}^i + \mathbf{E}_0{}^s) = 0$. The boundary condition is that $\Phi_0{}^i + \Phi_0{}^s$ must be constant on the surface $u_1 = u_{10}$, and without loss of generality, we can choose that constant to be zero. The solution to Laplace's equation in prolate spheroidal coordinates is [7]

$$\Phi(u_1,v_1,\phi) = \sum_{n=0}^{\infty}\sum_{m=0}^{n}[A_{nm}P_n{}^m(u_1) + B_{nm}Q_n{}^m(u_1)]$$
$$\cdot[C_{nm}P_n{}^m(v_1) + D_{nm}Q_n{}^m(v_1)][E_{nm}\sin m\phi + F_{nm}\cos m\phi] \quad (31)$$

where $P_n{}^m$ and $Q_n{}^m$ are associated Legendre functions of the first and second kinds, respectively. Since the boundary condition requires that

$$\Phi_0{}^i + \Phi_0{}^s = 0 \qquad \text{at the surface defined by } u_1 = u_{10}$$

$\Phi_0{}^s$ must have the same v_1 and ϕ dependence as $\Phi_0{}^i$. Hence we can choose one term out of the series in (31) which will satisfy the boundary condition. Accordingly, we set

$$\Phi_0{}^s = A_h \cos\phi P_1{}^1(v_1)Q_1{}^1(u_1) = A_h\cos\phi(1 - v_1{}^2)^{1/2}Q_1{}^1(u_1).$$

Since $Q_1{}^1(u_1) \to 0$ as $u_1 \to \infty$, this solution also satisfies the condition at infinity. Requiring $\Phi_0{}^i + \Phi_0{}^s$ to satisfy the boundary condition and solving for the constant A_h gives

$$A_h = l(u_{10}{}^2 - 1)^{1/2}/Q_1{}^1(u_{10})$$

and

$$\Phi_0{}^i + \Phi_0{}^s = -l\cos\phi(1 - v_1{}^2)^{1/2}[(u_1{}^2 - 1)^{1/2}$$
$$- (u_{10}{}^2 - 1)^{1/2}Q_1{}^1(u_1)/Q_1{}^1(u_{10})]. \quad (32)$$

To facilitate physical interpretation, we shall follow Van Bladel [7] and write $\mathbf{E}_1$ as the sum of two terms, $\mathbf{E}_1 = \mathbf{E}_1' + \mathbf{E}_1''$, where

$$\nabla\times\mathbf{E}_1' = 0 \quad (33)$$

$$\nabla\cdot\mathbf{E}_1' = 0 \quad (34)$$

$$\hat{\mathbf{n}}\cdot\sigma\mathbf{E}_1' = -\hat{\mathbf{n}}\cdot(\mathbf{E}_0{}^i + \mathbf{E}_0{}^s)/\eta_0 \qquad \text{on the surface} \quad (35)$$

$$\nabla\times\mathbf{E}_1'' = \eta_0\mathbf{H}_0 \quad (36)$$

$$\nabla\cdot\mathbf{E}_1'' = 0 \quad (37)$$

$$\hat{\mathbf{n}}\cdot\mathbf{E}_1'' = 0 \qquad \text{on the surface.} \quad (38)$$

Since the curl and divergence of $\mathbf{E}_1'$ are zero, $\mathbf{E}_1'$ can be found from $\mathbf{E}_1' = -\nabla\Phi_1'$ where Φ_1' satisfies Laplace's equation. Then the boundary condition given in (35) can be written, using the definition of the gradient, as

$$-\frac{1}{h_1}\frac{\partial\Phi_1'}{\partial u_1}\bigg|_{u_1=u_{10}} = -(1/h_1\sigma\eta_0)\frac{\partial}{\partial u_1}(\Phi_0{}^i + \Phi_0{}^s)\bigg|_{u_1=u_{10}}. \quad (39)$$

From this relation, it can be seen that Φ_1' must have the same v_1 and ϕ variation as $\Phi_0{}^i + \Phi_0{}^s$. Choosing the appropriate term from (31), we get

$$\Phi_1' = -B_h l\cos\phi(u_1{}^2 - 1)^{1/2}[(1 - v_1{}^2)]^{1/2}/\sigma\eta_0$$

where B_h is an arbitrary constant, and the $\sigma\eta_0$ term has been included for convenience. Requiring this to satisfy the boundary condition in (39) results in

$$B_h = 2[u_{10}{}^2 - 1]^{-1}[u_{10}{}^2/(u_{10}{}^2 - 1)$$
$$- (1/2)u_{10}\ln[(u_{10} + 1)/(u_{10} - 1)]]^{-1} \quad (40)$$

where we have used

$$Q_1{}^1(u_{10}) = (u_{10}{}^2 - 1)^{1/2}[u_{10}/(u_{10}{}^2 - 1)$$
$$- (1/2)\ln[(u_{10} + 1)/(u_{10} - 1)]] \quad (41)$$

$$\frac{d}{du_1}Q_1{}^1(u_1)\bigg|_{u_1=u_{10}} = [u_{10}{}^2 - 1]^{-1/2}[(u_{10}{}^2 - 2)/(u_{10}{}^2 - 1)$$
$$- (1/2)\ln[(u_{10} + 1)/(u_{10} - 1)]]. \quad (42)$$

Noting that Φ_1' in the preceding can be written as $\Phi_1' = -B_h x/\sigma\eta_0$, then $\mathbf{E}_1'$ can be written as

$$\mathbf{E}_1' = -B_h\hat{\mathbf{x}}/\sigma\eta_0 \quad (43)$$

where B_h is given by (40). This result is similar to that obtained for the sphere, where the electric field inside the sphere induced by the electric field of the incident wave is also uniform. Furthermore, it can be shown that $B_h \to 3$ as $u_{10} \to \infty$, and then (43) reduces to the value for a sphere (if the difference in polarization is accounted for). Note that since

$$u_{10} = a/(a^2 - b^2)^{1/2} \quad (44)$$

the limit as $u_{10} \to \infty$ corresponds to the limit as $b \to a$, which takes a spheroid into a sphere. The limit of (40) can be found without difficulty by first expanding the ln terms in an infinite series and then taking the limit.

It remains now to find the $\mathbf{E}_1''$ which satisfies (36)–(38). Since $\eta_0\mathbf{H}_0 = -\hat{\mathbf{z}}$,

$$\nabla\times\mathbf{E}_1'' = -\hat{\mathbf{z}}.$$

By inspection, a particular solution to this equation (in cylindrical coordinates) is

$$\mathbf{E}_1'' = -\frac{r\hat{\boldsymbol{\phi}}}{2}. \tag{45}$$

Since this also satisfies (37) and (38) ($\hat{\boldsymbol{\phi}}$ is parallel to the surface), it is the solution. In rectangular coordinates, $\mathbf{E}_1'' = (y\hat{\mathbf{x}} - x\hat{\mathbf{y}})/2$, and it is easy to see that this is equivalent to (19) for the sphere if the change in polarization is taken into account. Since the spheroid has the same kind of symmetry as the sphere when the magnetic field lies along the major axis of the spheroid, the interior electric field induced by the magnetic field has the same characteristics in the spheroid as in the sphere.

The electric field to first order inside the spheroid for magnetic polarization with the incident $\mathbf{E}$ in the x direction and incident $\mathbf{H}$ in the $-z$ direction is

$$\mathbf{E} = -jk(\mathbf{E}_1' + \mathbf{E}_1'') = B_h\hat{\mathbf{x}}[-j\sigma/\omega\epsilon_0]^{-1} - j\tfrac{1}{2}k(y\hat{\mathbf{x}} - x\hat{\mathbf{y}}) \tag{46}$$

with B_h given by (40). This expression will be used for power calculations in the next section.

B. Electric Polarization

Using the same orientation for the coordinate system with respect to the spheroid as shown in Fig. 2, the solution for electric polarization with the incident plane wave fields given by (18) and (19) is described next following the same basic approach used for magnetic polarization.

As in the two previous cases, $\mathbf{E}_0 = 0$, and since the spheroid is nonmagnetic, $\mathbf{H}_0 = \hat{\mathbf{x}}/\eta_0$. To find $\mathbf{E}_0^i + \mathbf{E}_0^s$, we can use

$$\mathbf{E}_0^i + \mathbf{E}_0^s = -\nabla(\Phi_0^i + \Phi_0^s) = -\nabla(-lu_1v_1 + \Phi_0^s)$$

since $\mathbf{E}_0^i = -\nabla(-z)$ and $z = lu_1v_1$. Since the boundary condition is again $(\Phi_0^i + \Phi_0^s) = 0$ when $u_1 = u_{10}$, Φ_0^s must have the same v_1 and ϕ variation as ϕ_0^i. Choosing the appropriate term from (31), we get

$$\Phi_0^s = A_e v_1 Q_1(u_1)$$

where A_e is a constant to be evaluated from the boundary conditions. Solving for A_e gives

$$A_e = lu_{10}/Q_1(u_{10})$$

and therefore

$$\Phi_0^i + \Phi_0^s = -lu_1v_1 + lu_{10}v_1Q_1(u_1)/Q_1(u_{10}). \tag{47}$$

Now $\mathbf{E}_1'$ can be found by solving (33)–(35) using $\mathbf{E}_1' = -\nabla\phi'$. As before, the boundary condition in (35) requires that Φ' have the same v_1 and ϕ dependence as $\Phi_0^i + \Phi_0^s$. Hence the appropriate form of Φ' as obtained from (31) is

$$\Phi_e' = -B_e lu_1v_1/\sigma\eta_0$$

where B_e is to be found from the boundary conditions. Solving for B_e from (35) gives

$$B_e = [u_{10}^2 - 1]^{-1}[(u_{10}/2)\ln[(u_{10}+1)/(u_{10}-1)] - 1]^{-1} \tag{48}$$

so that $\mathbf{E}_1'$ is given by

$$\mathbf{E}_1' = -B_e\hat{\mathbf{z}}/\sigma\eta_0 \tag{49}$$

since $lu_1v_1 = z$. Again it should be noted that since

$$\lim_{u_{10}\to\infty} B_e = 3$$

(49) reduces to the corresponding expression for a sphere.

The expression for $\mathbf{E}_1''$ is found by solving (36)–(38). For this polarization, (36) becomes

$$\nabla \times \mathbf{E}_1'' = \hat{\mathbf{x}}$$

which can be solved by setting

$$\mathbf{E}_1'' = y\hat{\mathbf{z}} - \nabla\Phi''$$

where $y\hat{\mathbf{z}}$ is a particular solution obtained by inspection, and Φ'' is a function which must satisfy Laplace's equation because $\nabla\cdot\mathbf{E}_1'' = 0$ and $\nabla\cdot y\hat{\mathbf{z}} = 0$. In addition, $\mathbf{E}_1''$ must satisfy the boundary condition given in (4),

$$\hat{\mathbf{u}}\cdot\mathbf{E}_1'' = y\hat{\mathbf{z}}\cdot\hat{\mathbf{u}} - \nabla\Phi''\cdot\hat{\mathbf{u}} = 0 \qquad \text{when } u_1 = u_{10} \tag{50}$$

where $\hat{\mathbf{u}}$ is a unit vector perpendicular to the surface of the prolate spheroid formed by $u_1 = u_{10}$. The quantity $y\hat{\mathbf{z}}\cdot\hat{\mathbf{u}}$ may be evaluated using $y = r\sin\phi$, (23), (25), and (28). The result is

$$y\hat{\mathbf{z}}\cdot\hat{\mathbf{u}} = (l/h_1)(u_1^2-1)^{1/2}(1-v_1^2)^{1/2}v_1\sin\phi$$

where

$$h_1 = (u_1^2 - v_1^2)^{1/2}/(u_1^2-1)^{1/2}.$$

(Note that this h_1 is the h_1 for the unnormalized coordinates (u,v,ϕ) as obtained from (28)–(30) written in terms of the normalized coordinates.) Consequently, the boundary condition in (50) requires

$$(1/h_1)(\partial\Phi'')\partial u_1) = (1/h_1)(u_1^2-1)^{1/2}(1-v_1^2)^{1/2}v_1\sin\phi \qquad \text{at } u_1 = u_{10}. \tag{51}$$

Thus Φ'' must have $(1-v_1^2)^{1/2}v_1\sin\phi$ variation, which may be obtained from the $m = 1$ terms in (31). Also since $P_2^1(v_1) = 3v_1(1-v_1^2)^{1/2}$, the $n = 2$ term is the appropriate one. Thus we choose a solution

$$\Phi'' = C_eP_2^1(u_1)P_2^1(v_1)\sin\phi$$

where C_e is a constant to be determined from the boundary condition in (51). Evaluating C_e and converting back to rectangular coordinates gives the final expression for $\mathbf{E}_1''$ for electric polarization

$$\mathbf{E}_1'' = u_{10}^2y\hat{\mathbf{z}}/(2u_{10}^2-1) + z\hat{\mathbf{y}}(1-u_{10}^2)/(2u_{10}^2-1). \tag{52}$$

Once again, as $u_{10}\to\infty$, $\mathbf{E}_1''$ reduces to the proper value for a sphere.

The electric field to first order inside the spheroid for electric polarization with the incident $\mathbf{E}$ in the z direction and the incident $\mathbf{H}$ in the x direction is

$$\begin{aligned}\mathbf{E} &= -jk(\mathbf{E}_1' + \mathbf{E}_1'') \\ &= B_e\hat{\mathbf{z}}[-j\sigma/\omega\epsilon_0]^{-1} - jk[u_{10}^2 y\hat{\mathbf{z}}/(2u_{10}^2 - 1) \\ &\quad + (1 - u_{10}^2)z\hat{\mathbf{y}}/(2u_{10}^2 - 1)] \end{aligned} \tag{53}$$

with B_e given by (48).

C. Cross Polarization

For cross polarization, the incident fields are chosen to be

$$\mathbf{E}^i = \hat{\mathbf{x}} \sum_{n=0}^{\infty} (-jkz)^n/n!$$

$$\mathbf{H}^i = (\hat{\mathbf{y}}/\eta_0) \sum_{n=0}^{\infty} (-jkz)^n/n!.$$

Following the same procedure as described in the preceding for magnetic polarization and electric polarization results in the following expressions for $\mathbf{E}_1'$ and $\mathbf{E}_1''$

$$\mathbf{E}_1' = -B_c\hat{\mathbf{x}}/\sigma\eta_0 \tag{54}$$

$$\mathbf{E}_1'' = u_{10}^2 x\hat{\mathbf{z}}/(1 - 2u_{10}^2) - (u_{10}^2 - 1)z\hat{\mathbf{x}}/(1 - 2u_{10}^2) \tag{55}$$

where

$$\begin{aligned}B_c &= 2(u_{10}^2 - 1)^{-1}[u_{10}^2/(u_{10}^2 - 1) \\ &\quad - (u_{10}/2)\ln[(u_{10} + 1)/(u_{10} - 1)]]^{-1}.\end{aligned} \tag{56}$$

Note that $B_c = B_h$ since, in each case, the electric field is perpendicular to the major axis. The electric field inside the spheroid to first order for this cross polarization is then

$$\begin{aligned}\mathbf{E} &= -jk(\mathbf{E}_1' + \mathbf{E}_1'') \\ &= B_c\hat{\mathbf{x}}[-j\sigma/\omega\epsilon_0]^{-1} - jk[u_{10}^2 x\hat{\mathbf{z}}/(1 - 2u_{10}^2) \\ &\quad - (u_{10}^2 - 1)z\hat{\mathbf{x}}/(1 - 2u_{10}^2)].\end{aligned} \tag{57}$$

Having thus obtained the first-order electric fields inside the spheroid for each of the principal polarizations, we can now proceed to calculate the power absorbed by the spheroid.

IV. ABSORBED POWER CALCULATIONS

With the expressions for the first-order interior fields that were obtained in the previous section, the first-order calculation of the absorbed power density and the absorbed total power inside the spheroid is straightforward. The time-average absorbed power density is given by

$$\mathcal{P} = \tfrac{1}{2}\sigma\mathbf{E}\cdot\mathbf{E}^* \tag{58}$$

and the total time-average absorbed power is given by the volume integral

$$P = \int_V \mathcal{P}\,dV = \int_{-a}^{a}\int_0^{2\pi}\int_0^{f(z)} \mathcal{P}r\,dr\,d\phi\,dz \tag{59}$$

where

$$f(z) = (b^2 - b^2z^2/a^2)^{1/2}.$$

The integral has been written in terms of cylindrical coordinates because the integration is easier in cylindrical coordinates.

Using in turn (46), (53), and (57) in (58) gives the following expressions for power densities for magnetic, electric, and cross polarizations, labeled $\mathcal{P}_h$, $\mathcal{P}_e$, and $\mathcal{P}_c$, respectively

$$\mathcal{P}_h = \tfrac{1}{2}\sigma k^2[(B_h/\sigma\eta_0)^2 - (B_h/2\sigma\eta_0)r\sin\phi + r^2/4] \tag{60}$$

$$\begin{aligned}\mathcal{P}_e &= \tfrac{1}{2}\sigma k^2[(B_e/\sigma\eta_0)^2 - 2B_e a^2 r\sin\phi/\sigma\eta_0(a^2 + b^2) \\ &\quad + a^4r^2\sin^2\phi/(a^2 + b^2)^2 + b^4z^2/(a^2 + b^2)^2]\end{aligned} \tag{61}$$

$$\begin{aligned}\mathcal{P}_c &= \tfrac{1}{2}\sigma k^2[(B_c/\sigma\eta_0)^2 - 2B_c b^2 z/\sigma\eta_0(a^2 + b^2) \\ &\quad + b^4z^2/(a^2 + b^2)^2 + a^4r^2\cos^2\phi/(a^2 + b^2)^2]\end{aligned} \tag{62}$$

where (44) has been used and the conversion to cylindrical coordinates has been made. The integration to find the total time-average absorbed power density is straightforward and gives the following results

$$P_h = \tfrac{1}{2}\sigma k^2[(B_h/\sigma\eta_0)^2 + b^2/10](4/3)\pi ab^2 \tag{63}$$

$$P_e = \tfrac{1}{2}\sigma k^2[(B_e/\sigma\eta_0)^2 + a^2b^2/5(a^2 + b^2)](4/3)\pi ab^2 \tag{64}$$

$$P_c = \tfrac{1}{2}\sigma k^2[(B_c/\sigma\eta_0)^2 + a^2b^2/5(a^2 + b^2)](4/3)\pi ab^2. \tag{65}$$

Some of the power absorption characteristics are shown in the curves in Figs. 4 and 5. Fig. 4 shows the average absorbed power density (total power absorbed divided by the volume) for each polarization along with that absorbed by a sphere P_s, as a function of frequency for the indicated parameters. The expression for P_s is obtained by integrating (20) and is

$$P_s = \tfrac{1}{2}\sigma k^2[(3/\sigma\eta_0)^2 + r_0^2/10](4/3)\pi r_0^3 \tag{66}$$

where r_0 is the radius of the sphere. The calculations are made for the case where the spheroid and sphere have equal volumes, i.e., $(4/3)\pi ab^2 = (4/3)\pi r_0^3$, and for an incident power density of 1 mW/cm^2. The dimensions of the spheroid are chosen so that the size of the spheroid approximates that of a man and the conductivity and permittivity used for human tissue are those given by Johnson and Guy [1] and Schwan [9].

Lin *et al.* [5] demonstrated from the Mie solution for a sphere that power absorption due to the incident electric and magnetic fields can be identified separately. For the prolate spheroid, an additional cross product term appears, but we will use the concept of power absorption induced separately by incident E and H fields in the arguments which follow. It is interesting to note that the power absorbed for electric polarization is higher than that of the corresponding sphere, while for cross polarization and magnetic polarization, it is lower. There is a factor of five to ten difference in the power absorbed for electric polarization compared to magnetic polarization for the conditions of Fig. 4.

For electric polarization, the incident electric field is tangential to the long axis of the spheroid, and the field boundary conditions thus require the magnitude of the

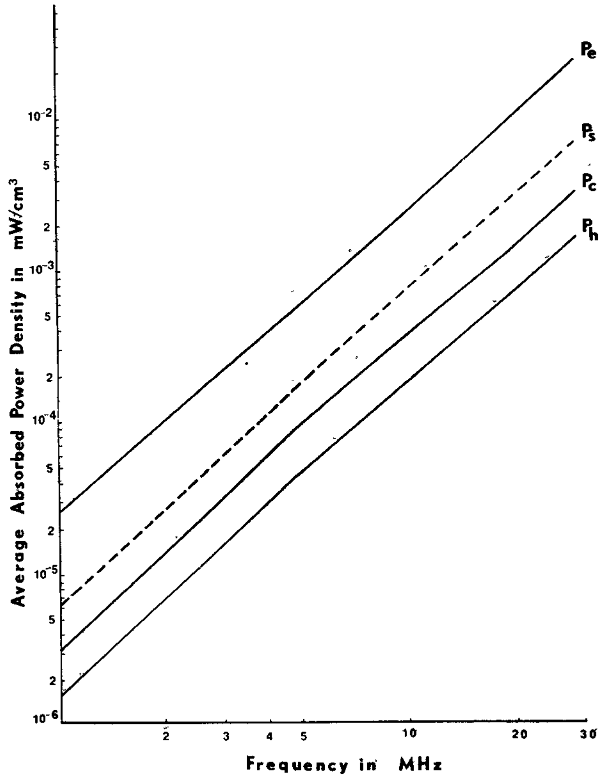

Fig. 4. Average absorbed power density by a muscle prolate spheroid for each of the three polarizations, electric (P_e), magnetic (P_h), and cross (P_c), and for a sphere (P_s) with an incident power density of 1 mW/cm², $a = 1$ m, $a/b = 7.73$, volume = 0.07 m³.

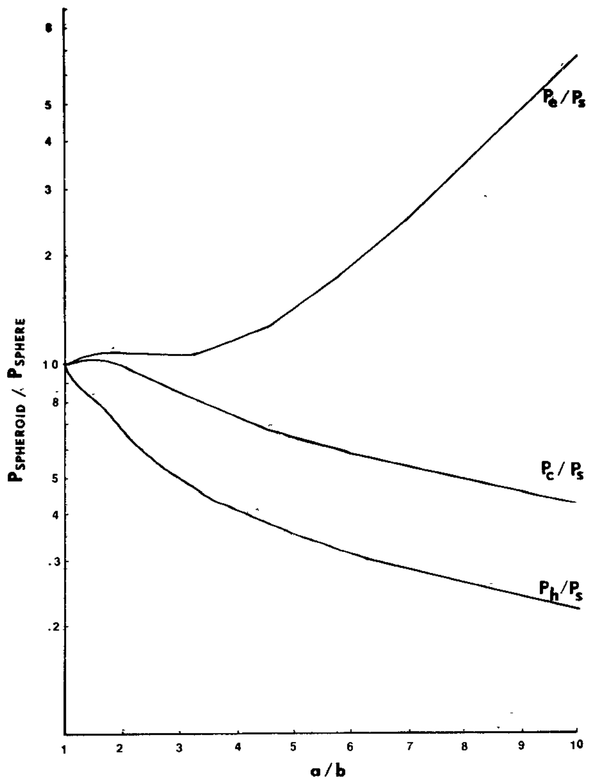

Fig. 5. Total absorbed power of a 0.07-m³ muscle prolate spheroid normalized to that of a muscle sphere of equal volume for each of the polarizations as a function of the ratio of the major axis to the minor axis of the spheroid at 10 MHz.

internal electric field to approach that of the incident electric field. For cross or magnetic polarization, the incident electric field is perpendicular to the long axis of the spheroid, and the field boundary conditions require the internal electric field to be reduced by a factor like $1/(\epsilon_r + \sigma/j\omega\epsilon_0)$, which is a small number. Thus the incident electric field is strongly coupled into the spheroid only for electric polarization. The internal electric field induced by the incident magnetic field forms loops about the incident magnetic field vector and increases in strength with the amount of incident magnetic flux intercepted by the spheroid. Hence the magnetically induced internal electric field is stronger for electric and crosspolarization, where the incident magnetic field is along the minor axis and more magnetic flux is intercepted, than it is for magnetic polarization. Consequently, P_e is greatest because of strong electric and strong magnetic field coupling, P_c is intermediate because of strong magnetic coupling but weak electric coupling, and P_h is smallest because of weak electric and weak magnetic field coupling.

If this qualitative explanation is correct, the differences between P_e, P_c, and P_h should increase as the spheroid becomes longer and thinner. This does happen as shown by the curves in Fig. 5, where the total absorbed power for each polarization is shown normalized to the total power absorbed by a sphere of equal volume and plotted against the ratio a/b.

These results are in good qualitative agreement with measurements of power absorbed by a saline-filled rectangular box in a large transmission line which simulates a plane wave, made by Allen [10], and with measurements of power absorbed by prolate spheroid phantom tissue models in a transmission line, made by Gandhi [11].

V. SUMMARY AND CONCLUSIONS

Perturbation techniques have been applied to obtain the first-order internal electric fields and absorbed power for plane wave irradiation of a prolate spheroid model of man when the wavelength is long compared to the dimensions of the spheroid. Power calculations based on these results show a striking change in absorbed power with a change in orientation of the spheroid in the incident fields.

The expressions for absorbed power density and absorbed total power should prove to be very useful in studies of radiation hazards to man. For example, the results of this analysis clearly indicate the importance of the incident magnetic field and of the orientation of the absorbing body in the incident fields with respect to the power absorbed. Another very important application will be in the extrapolation of the results of animal experiments involving radiation effects to man. Since the absorbed power in a given radiation field varies with the size of the absorbing body, in extrapolating animal effects to man it will be necessary to relate the biological effects to the internal fields or power absorption and then relate the internal fields or power absorption to the incident fields. This kind of analysis should be very valuable in establishing such relations for the long-wavelength case.

There are many directions in which this analysis might be extended, some of which are in progress. One extension would be to that of the power absorbed by an object in near fields, rather than plane wave fields. Another is to analyze the power absorbed by an oblate spheroid, which is a better model of some animals, such as the turtle and perhaps the rabbit, than the prolate spheroid. Also the oblate spheroid analysis could be applied to the power absorbed by some kinds of cells. Another application might be the calculation of power distribution in a physiological solution containing cells in a petri dish. The range of frequency for which the results are valid should be examined carefully, and the possibility of increasing the range of validity through higher order terms explored. Verification of the analysis should be made through careful measurements.

REFERENCES

[1] C. C. Johnson and A. W. Guy, "Nonionizing electromagnetic wave effects in biological materials and systems," *Proc. IEEE*, vol. 60, pp. 692–718, June 1972.

[2] A. Anne, M. Satio, O. M. Salati, and H. P. Schwan, "Relative microwave absorption cross sections of biological significance," in *Biological Effects of Microwave Radiation Proc. 4th Tri-Service Conf. on the Biological Effects of Microwave Radiation* (New York Univ. Medical Center, N. Y.), M. F. Peyton, Ed., vol. 1. New York: Plenum, 1960, pp. 153–176.

[3] A. R. Shapiro, R. F. Lutomirski, and H. T. Yura, "Induced fields and heating within a cranial structure irradiated by an electromagnetic plane wave," *IEEE Trans. Microwave Theory Tech. (Special Issue on Biological Effects of Microwaves)*, vol. MTT-19, pp. 187–196, Feb. 1971.

[4] H. N. Kritikos and H. P. Schwan, "Hot spots generated in conducting spheres by electromagnetic waves and biological implications," *IEEE Trans. Bio-Med. Eng.*, vol. BME-19, pp. 53–58, Jan. 1972.

[5] J. C. Lin, A. W. Guy, and C. C. Johnson, "Power deposition in a spherical model of man exposed to 1–20-MHz electromagnetic fields," *IEEE Trans. Microwave Theory Tech. (1973 Symposium Issue)*, vol. MTT-21, pp. 791–797, Dec. 1973.

[6] W. T. Joines and R. J. Spiegel, "Resonance absorption of microwaves by the human skull," *IEEE Trans. Bio-Med. Eng.*, vol. BME-21, pp. 46–48, Jan. 1974.

[7] J. Van Bladel, Electromagnetic Fields. New York: McGraw-Hill, 1964.

[8] M. R. Spiegel, *Mathematical Handbook of Formulas and Tables (Schaum's Outline Series)*. New York: McGraw-Hill, p. 124, 1968.

[9] H. P. Schwan, "Electrical properties of tissues and cells," *Advan. Biol. Med. Phys.*, vol. 5, pp. 147–209, 1957.

[10] S. J. Allen, "Measurements of power absorption by human phantoms immersed in radio frequency fields," presented at the New York Academy of Sciences Conf. on the Biological Effects of Nonionizing Radiation, New York, Feb. 12–15, 1974.

[11] O. P. Ghandi, "A method of measuring RF absorption of whole animals and bodies of prolate spheroidal shapes," in *Proc. of the 1974 Microwave Power Symp.* (Milwaukee, Wis.), May 28–31, 1974.

Short Papers

Design Equations for an Interdigitated Directional Coupler

WEN PIN OU, MEMBER, IEEE

***Abstract*—General design equations for an interdigitated directional coupler are derived. The design equations are written in terms of even- and odd-mode admittances for a pair of coupled lines which are identical to any pair of adjacent lines in the coupler. The calculated values of even- and odd-mode admittances can be translated into a physical configuration from published data on coupled lines.**

I. INTRODUCTION

Because of the advantages of broad-band, low loss, and tight coupling available in simple planar structures, the use of interdigitated structure as a directional coupling scheme has gained popularity among design engineers in recent years. Lange [1] first reported a 3-dB interdigitated microstrip hybrid in 1969. Later, in 1972, Waugh and LaCombe [2] constructed an "unfolded" version of a 3-dB Lange coupler and demonstrated that the performance is essentially the same as that of the Lange coupler, thus providing flexibility in geometrical layout of microstrip circuits. The extension of the interdigitated structure to a more loosely coupled directional coupler was recently reported by Miley [3].

Manuscript received May 14, 1974; revised July 26, 1974.
The author is with the Semiconductor Products Division, Motorola, Inc., Phoenix, Ariz. 85008.

While the circuit has been fabricated and put into practical applications, unfortunately no general design method for interdigitated couplers has been published. Thus a designer is forced to use a trial-and-error approach to achieve his design objective. This short paper attempts to fill this gap by giving a theoretical treatment of the interdigitated structure. General design equations for a directional coupler are derived, which, in turn, can be translated into a physical configuration by using published data available in the literature.

II. ARRAY OF PARALLEL—COUPLED LINES

Consider first an array of k parallel-coupled TEM lines as shown in Fig. 1. It is assumed that the physical dimensions of each line are identical, so are the spacings between the lines. The total number of lines k is assumed to be even. Generally, there are couplings in existence between any pair of lines. However, for mathematical simplicity and practical consideration, only the couplings between the adjacent lines will be considered. The neglect of nonadjacent couplings is not a serious limitation in many practical applications, as pointed out by Matthaei [4]. Though not exact, the assumption of TEM mode provides good approximation for microstrip, as will be seen later from comparison of theoretical results and empirical data.

The current and voltage relation for such an array of transmission lines may be written as follows:

$$I_{ma} = -j\cot\theta \sum_{n=m-1}^{m+1} Y_{mn}V_{na} + j\csc\theta \sum_{n=m-1}^{m+1} Y_{mn}V_{nb} \qquad (1)$$